Class III alcohol dehydrogenase: consistent pattern complemented with the mushroom enzyme

Annika Norin[1], Jawed Shafqat[1], Mustafa El-Ahmad, Gunvor Alvelius, Ella Cederlund, Lars Hjelmqvist, Hans Jörnvall*

Department of Medical Biochemistry and Biophysics, Karolinska Institutet, SE-171 77 Stockholm, Sweden

Received 18 November 2003; revised 18 December 2003; accepted 20 December 2003

First published online 21 January 2004

Judit Ovádi

Abstract Mushroom alcohol dehydrogenase (ADH) from *Agaricus bisporus* (common mushroom, champignon) was purified to apparent homogeneity. One set of ADH isozymes was found, with specificity against formaldehyde/glutathione. It had two highly similar subunits arranged in a three-member isozyme set of dimers with indistinguishable activity. Determination of the primary structure by a combination of chemical, mass spectrometric and cDNA sequence analyses, correlated with molecular modeling towards human ADHs, showed that the active site residues are of class III ADH type, and that the subunit differences affect other residues. Class I and III forms of ADHs characterized define conserved substrate-binding residues (three and eight, respectively) useful for recognition of these enzymes in any organism.

Key words: Alcohol dehydrogenase class I and III; Isozyme; Pattern recognition; Active site; Mushroom enzyme

1. Introduction

Alcohol dehydrogenases (ADHs) illustrate several types of evolutionary changes in proteins. The first ADH structure determined was one of the dehydrogenase structures that helped to establish the widespread occurrence of a common nucleotide-binding fold [1,2]. Also early, relationships were established between the tetrameric and dimeric ADHs [3], both now known to be members of the MDR (medium-chain dehydrogenases/reductases) superfamily [4]. Presently, at least five superfamilies have been found to give rise to ADH activity (recent summary in [5]).

The first known family with ADH activity (MDR) is now known to have evolved into minimally 23 forms in the human genome [4,5], giving rise also to class and isozyme subforms. The gene duplications have been traced, in particular the major division into two functionally separate lines of ADH, class III (the ancestral [6] glutathione-dependent formaldehyde dehydrogenase [7]) and several non-III classes with emerging ethanol-related activities. This line separation has been dated to 500 million years ago [8], giving rise to enzymes with closely similar folds but highly different in evolutionary rate of changes (3–5-fold faster in non-class III) and in pattern of local regions affected [9]. To establish these relationships, MDR ADH has been characterized in most major life forms, ranging from bacteria and archaea to eukaryotes of plants, yeasts, insects, animals and the human [8]. In this long-term study, two bacterial, special ADH forms, mycothiol-dependent ADH and a nicotinoprotein ADH, were found to occupy evolutionary positions intermediate between those of the 'dimeric ADH' family and those of other MDR families [10,11]. In spite of the many forms, the enzyme characteristics of several lines, including that for the enzyme from mushroom, have not been established. We now report purification, properties, and structural relationships of this ADH line, too. Together with previous data, the present structure defines further relationships, establishes the constant pattern, and defines the type of residue variability at the active site.

2. Materials and methods

2.1. Purification, multiplicity, and assays

Agaricus bisporus mushroom (1 kg) was used for purification of ADH. The material was homogenized, centrifuged and precipitated with 65% ammonium sulfate. The precipitate was dissolved in 20 mM Tris/HCl, pH 8.8, dialyzed against the same buffer and applied onto an anion diethylaminoethyl (DEAE) fast flow column (50 mM Tris/HCl, pH 8.8). All buffers used throughout the purification contained 0.1 mM dithiothreitol. The product was eluted with a gradient of 0–0.5 M NaCl in the same buffer. After dialysis of the eluted activity in 20 mM phosphate buffer, pH 7.5, the sample was loaded onto adenosine monophosphate (AMP)-Sepharose (20 mM phosphate buffer, pH 7.5) and eluted with a gradient of 0–3.6 mM oxidized nicotinamide adenine dinucleotide (NAD^+) in the same buffer. The active fractions were pooled, dialyzed against 20 mM Tris/HCl, pH 8.8, applied onto Mono-Q fast protein liquid chromatography (FPLC) (Amersham Biosciences) and eluted with a gradient of 0–0.5 M NaCl in the same buffer. The fraction containing ADH activity was dialyzed and applied to a chromatofocusing Mono-P FPLC column in 25 mM Tris/HCl, pH 7.1, and eluted with 25 mM polybuffer 74 (Amersham Biosciences), which gave rise to three activity peaks, equidistantly separated. Throughout purification the enzyme was traced by glutathione-dependent formaldehyde activity measurements [12] once class III had been established to be the activity present. Protein contents were determined using colorimetric methods [13]. The three forms were analyzed by native gel electrophoresis and stained for activity and protein as described [12].

2.2. Primary structure analysis

The purified protein was analyzed by peptide generation in separate batches using *Achromobacter* Lys-specific (Waco), *Staphylococcus*

*Corresponding author. Fax: (46)-8-33 74 62.
E-mail address: hans.jornvall@mbb.ki.se (H. Jörnvall).

[1] These authors contributed equally to this work.

Abbreviations: ADH, alcohol dehydrogenase; MDR, medium-chain dehydrogenase/reductase

0014-5793/04/$30.00
doi:10.1016/S0014-5793(03)01524-2

Glu-specific (Roche Diagnostics) and *Pseudomonas* Asp-specific proteases (Roche Diagnostics). The peptides were separated by reverse phase high performance liquid chromatography (HPLC) [12] and analyzed by N- and C-terminal sequencer degradations (Applied Biosystems) and by matrix-assisted laser desorption/ionization (MALDI) mass spectrometry. Remaining parts (except the very N-terminus) were analyzed via cloning of mushroom cDNA using reverse transcription-polymerase chain reaction (RT-PCR) to yield a structure which also confirmed most of the peptide-analyzed parts. Finally, the acetylated N-terminus and the subsequent 26 residues were determined by collision-induced dissociation (CID) fragmentation of two N-terminal peptides in a Q-time-of-flight (TOF) mass spectrometer (Micromass). Ile/Leu are indistinguishable by the mass spectrometry used and occur at two positions (positions 4 and 8). Both were assigned as Ile from the total compositions of the peptides and from direct sequence analysis after deacetylation in trifluoroacetic acid (TFA)/methanol (1:1, by vol) at room temperature for 18 h [14].

Total RNA was purified using the RNeasy plant minikit (Qiagen). First-strand cDNA synthesis was performed by RT-PCR using Superscript II (Invitrogen), utilizing 4.2 μg RNA. Primers designed from the DNA sequence of phosphoglycerate kinase in *A. bisporus* were used as a positive control. Degenerated primers were designed from the peptide sequence of *A. bisporus* using the program GeneFisher [15]. Inosine was used in those cases where there was a choice of four nucleotides in the last position of the triplet codon. The PCR was run on a MiniCycler (MJ Research) in a 50 μl scale using platinum *Taq* DNA polymerase high fidelity (Invitrogen) with hot start and an annealing temperature of 60°C. The PCR product was purified using the QIAquick gel extraction kit from Qiagen and cloned into a TOPO TA vector (Invitrogen) using the TOPO TA cloning kit for sequencing. Plasmid DNA was purified using the GFX microplasmid prep kit (Amersham Biosciences). The DNA of interest was sequenced using the DYEnamic ET terminator cycle sequencing kit (Amersham Biosciences) at the Center for Genomics and Bioinformatics, Karolinska Institutet. Using the GeneRacer kit (Invitrogen) with gene-specific primers, the whole coding region except the first 225 bases in the 5′-end could be established.

2.3. Alignments, modeling and calculations

Sequence alignments and phylogenetic relationships were evaluated using the program CLUSTAL W [16] with bootstrap analysis [17]. Molecular modeling was performed with the program ICM (version 2.7; Molsoft LLC) with the known structure of human class III ADH (1MC5 [18]) as template. In this procedure, aligned residues were tethered to the template structure and relaxed by energy refinements. Deletions and gaps were modeled by biased probability Monte Carlo simulation [19]. The conformation of the coenzyme and the substrate was taken from the template.

3. Results

ADH from common mushroom was purified by a four-step chromatographic method similar to that for other MDR ADHs. The final product revealed the presence of a three-fraction isozyme set, as detected by electrophoresis under native conditions, suggesting that the enzyme is composed of two subunits (A and B) in all possible dimer combinations (Fig. 1). Evaluation of all three components (AA, AB and BB) by sodium dodecyl sulfate–polyacrylamide gel electrophoresis (SDS–PAGE) showed in each case a subunit size of about 40 kDa (mass from the sequence is 40.0 kDa). Activity staining after PAGE under native conditions showed each fraction to have a strong activity with glutathione/formaldehyde, and consistently, the crude extract had only weak activity with ethanol. No other ADH-active fractions were observed during the purification. The results indicate the presence of one major ADH set of three dimers and show that all have specific activities of about 32 U/mg with formaldehyde/glutathione as substrate.

The primary structure was established by a mixed approach, using chemical/mass spectrometric/cDNA sequence analysis. First, the homogeneous material in fractions AA and BB was individually digested with proteolytic enzymes and the resulting peptides were purified with reverse phase HPLC for sequencer analysis. The AA and BB material gave highly similar peptide patterns, and the sequencer analyses of the peptides showed no positions with microheterogeneities. In all, 27 peptides were chemically analyzed, giving the structure of final residues 1–98 and 224–378. Peptides, also including segments later identified via cDNA information (below), were analyzed by MALDI mass spectrometry, verifying correct molecular weights in each case tested. Two N-terminally blocked peptides were analyzed for sequence by CID fragmentation in a Q-TOF mass spectrometer and by chemical sequencer degradation after deblocking in TFA/methanol. The structures established the acetylated N-terminus of the intact protein, recovered in an 11-residue fragment after Lys-protease digestion and a 27-residue fragment after Asp-protease digestion (Fig. 2).

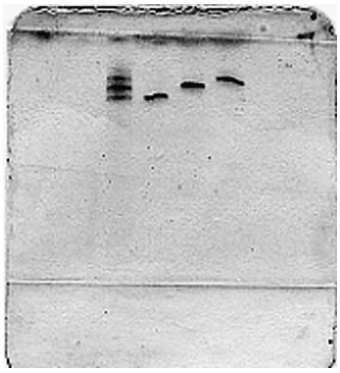

Fig. 1. Native PAGE of the three isozyme fractions obtained in the final purification step (right three lanes) and the unseparated isozyme mixture from the previous step (left lane).

The peptide structures obtained were used for design of degenerate oligonucleotide primers to amplify a cDNA fragment using RT-PCR of mushroom RNA. The 3′ cDNA fragment was amplified using internal primers and a modified oligo dT primer (of Invitrogen GeneRacer). The very 5′ cDNA fragment could not be amplified in spite of many attempts. However, the peptide segments initially recovered were amply joined and the complete primary structure thus established, showing a 378-residue native polypeptide subunit (Fig. 2). Microheterogeneities were detected at three positions, a Ser/Pro exchange at position 194, a Val/Leu exchange at position 335 and a Ser/Arg exchange at position 353 (Fig. 2). Although determined from the cDNA analyses via the PCR approach, they are considered reliable and derived from the native structure, since they were obtained repeatedly with three different sets of primers/PCRs, and since the subunit charge difference detected (the Ser/Arg exchange at position 353) is compatible with separate electrophoretic mobilities during enzyme purification as observed during the initial ADH purification (Fig. 1). It is concluded that the combined sequence results obtained establish the general nature of both subunits A and B, and that the corresponding gene structures are present in one organism. The latter follows from the fact that heterodimeric ADH is stable during the purification steps used, as demonstrated with many ADH forms [24] and by lack of isozyme regenerations during purification (Fig. 1, mid-

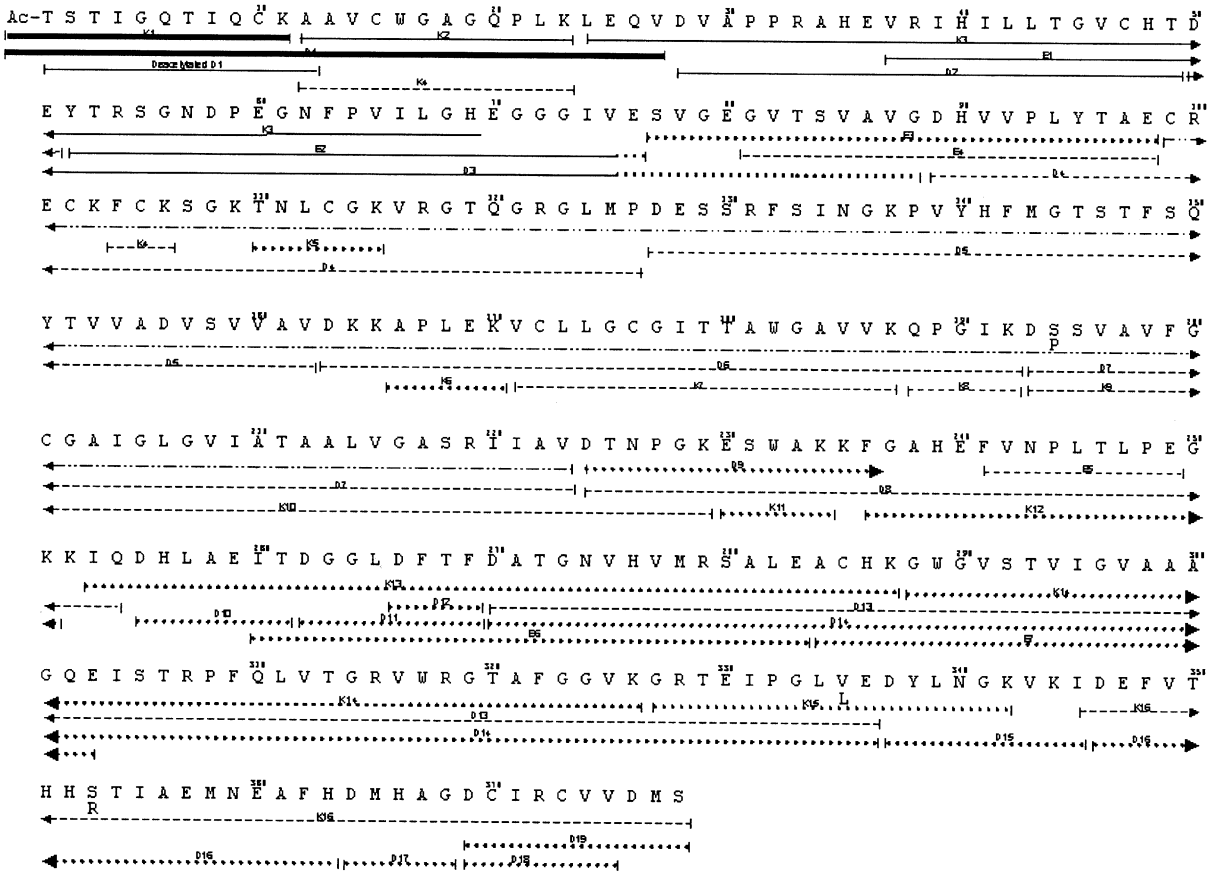

Fig. 2. Primary structure of mushroom ADH III and experimental proof obtained. Thin line, results from chemical sequencer degradations; dash-dotted line, from cDNA analysis; dotted line, from both protein and cDNA sequence analysis; thick line, from CID mass spectrometry; dashed line, from verification by MALDI peptide analysis. Microheterogeneities at positions 194, 335 and 353 are indicated by two residue alternatives.

dle of the three right lanes). The primary structure of mushroom ADH is 60% identical to that of human class III ADH and only about 45% identical to those of human non-class III ADHs, establishing the mushroom enzyme as a class III ADH, in agreement with the activity data. Combination of the aligned sequences of this and other MDR ADHs in a phylogenetic tree [20] also demonstrates that the present structure constitutes a branch of the III tree, most closely related to the MDR ADHs of the yeasts *Saccharomyces cerevisiae* (60% identical), *Schizosaccharomyces pombe* (57%) and *Pichia pastoris* (65%). Hence, all analyses agree with the assignment from the activity estimates during purification.

The primary structure obtained was further modeled by the ICM program into the three-dimensional structure of human class III ADH as reported from crystallographic analyses [18]. The results obtained show that the present structure is possible to adopt into a conformation closely related to that of the class III enzyme. Root mean square deviations from the human ADH III form are only 0.34 Å for the α-atoms. The close agreements of the substrate-binding residues at the active site are shown in Fig. 3. These modeling experiments support the class III assignment of the detectable ADH in the mushroom tissue.

With the present identification of the major mushroom ADH as a class III form, the structural variability at the substrate-binding site is known for a large number of MDR

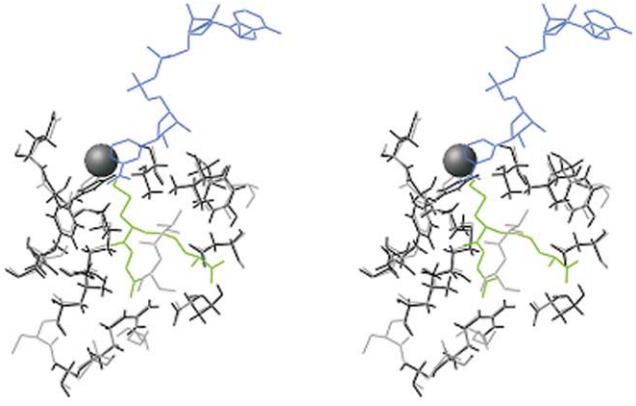

Fig. 3. Conformational relationships at the active site of the MDR class III ADHs. The residues shown are those within a distance of 3.8 Å of the substrate. Gray residues, human enzymes as determined by crystallographic analysis [18]; black residues, mushroom residues as modeled using the ICM program. Alignment between the two species forms shows two residue replacements at the active site as given in Table 1 (positions 93 and 111). Three gray residues are shown without modeled counterpart residues since they belong to the other subunit not modeled. The two zinc atoms are shown space-filled (cpk) in gray. The coenzyme is shown in blue and hydroxymethyl-glutathione in green.

Table 1
Residue variability at the substrate-binding positions of class III ADHs

Source ADH3	Substrate-binding positions																	
	HMGSH site							Anion site			Active site lining							
	46	49	55	57	66	67	294	111	114	283	92	93	109	140	293	308	309	317
Human	**T**	**Y**	**D**	**E**	**H**	**E**	**A**	**Q**	**R**	**K**	**Y**	I	**L**	**M**	**V**	**V**	**T**	**A**
Horse												I						
Rabbit												I						
Mouse												I						
Rat												I						
Uromastix												I						
Hagfish												I						
Octopus												V						
Drosophila		F										I					V	
Amphioxus												I						
Caenorhabditis elegans												V						
Sea bream												V						
Cod h												V						
Cod l												V						
Pufferfish a												V						
Pufferfish b												I						
Pea								G				Q						
Arabidopsis thaliana								G				Q						
Rice								G				Q						
Maize								G				Q						
S. pombe								S				**T**						
S. cerevisiae								G										
Mushroom								G										
P. pastoris								G										
Hordeum vulgare			G	T				D			F			V				
Potato			G	N				S			F		M	V				
Petunia			G	N				S			F		M	V				
Yersinia pestis																		
Pseudomonas aeruginosa																		
Escherichia coli		F						V		R								
Neisseria meningitidis		F						V		R								
Salmonella typhimurium		F																
Caulobacter crescentus								T		R								
Rhodobacter sphaeroides		F						T		R								

Positions are assigned from the crystallographically determined human enzyme [18] and residues obtained by alignment of fully analyzed class-ascribed ADH sequences in data banks. Bold letters indicate the majority assignment, and empty spaces that the residues are identical to the majority assignment. As shown, eight positions (46, 66, 67, 114, 293, 294, 308, 317) have thus far strictly conserved residue assignments, and remaining positions restricted variability.

ADHs from different life forms. The substrate-binding residues, as defined from the crystallographically determined tertiary structure of the human class III ADH enzyme [18] are given in Table 1, and compared to those similarly established in class I ADH of the horse and human enzymes [21,22]. As shown, patterns are completely different and highly typical in each case. Among presently analyzed and clearly assigned forms (34 for class III and 25 for class I, cf. Tables 1 and 2), class I has three positions (H67, E68 and F140) and class III eight positions (T46, H66, E67, A294, R114, V293, V308, A317) with thus far strictly conserved residues. In addition, the variability at further residues is limited (cf. Tables 1 and 2). These patterns establish the type of structures of each of these major ADH classes, and can be used for direct assignments of any ADH from future gene analyses as to class I (i.e. main class of 'recent' evolutionary origin [9] with ethanol activity) or class III (i.e. 'ancient' form [9] with activity against glutathione-coupled formaldehyde).

4. Discussion

The present analyses define the nature of mushroom ADH. Although the overall relationships were not unexpected, the isozyme occurrence was unexpected and the class assignment is relevant in the sense that it helps to complete the set of known forms from highly different branches of this model enzyme. For ADH, the class III presence is established in several major branches of not only animal but also plant and now fungal lines (Table 1). The patterns known (Tables 1, 2) can safely identify the functional activity as to class I or III of any MDR ADH detectable in future genome analyses.

The presence of multiple forms in class III is noteworthy, independent of whether they are allelozymes or derived from separate loci, since ADH isozymes were originally considered typical of the variable and more rapidly evolving class I forms, where isozymes have been known since long [23]. A few isozyme cases have been seen in class III before, but then appeared to be associated with special properties or activity differences [24]. The present data show that isozyme patterns are not unique to the classes, and that the classical tripartite isozyme pattern of class I can occur in the class III forms (Fig. 1) as also found in lower vertebrates (cartilaginous fish; Shafqat et al., unpublished). Furthermore, the limited difference between the isozyme forms now defined through cDNA sequence analysis is compatible with the fact that the isozyme differences were not detected by the peptide analyses.

Table 2
Residue variability at the substrate-binding positions of class I ADHs

Source ADH1	Substrate-binding positions													
	Inner part of pocket						Middle					Outer		
	48	67	68	93	140	141	57	115	116	294	318	110	306	309
Human γ	**S**	**H**	**E**	**F**	**F**	V	**L**	**D**	**L**	**V**	I	Y	**M**	**L**
Human β	T					**L**					V	Y		
Human α	T			A			M		V		I	Y		
Monkey	T			A			M		V			Y		
Baboon	T					V						Y		
Horse S								–			I	L		
Horse E											I	F		
Rabbit						I	I				I	F		
Deer mouse						I					I			
Mouse						I					I	F		
Rat						I		K			I			
Gopher B.M.							I							
Gopher K.							I							
Gopher T.							I							
Uromastix a						I	F			L			G	F
Uromastix b						V		E				V	L	F
Cobra						I	F						L	F
Alligator						I								F
Kiwi						I			I					F
Ostrich						A			I					F
Quail						I								F
Chicken						V								F
Frog									I	L			L	
Cod	T						K	W	A	W	M	Q	I	I
Pufferfish	T						K	A	N	W	Y	H	E	L

Positions are as reported from the crystallographically determined horse and human enzymes [21,22] and as obtained by alignment to fully analyzed class-ascribed ADH sequences in data banks. Bold letters and empty spaces as in Table 1. As shown, only three positions (67, 68, 140) are thus far strictly conserved in class I, but variability is restricted at all positions. Gopher B.M. indicates the species *Geomys bursarius major*, Gopher K. *Geomys knoxjonesi*, and Gopher T. *Geomys texensis*.

Finally, as a methodological point, the present data establish that complete ADH structural information can be readily obtained by combined use of separate techniques. Traditionally, mid-segment sequence portions of ADH have been difficult to recover because of low yield of large, hydrophobic peptides from this segment, and were missed in sequencer analysis also now (Fig. 2). The N-terminal portions, on the other hand, are often acetyl-blocked [25], as now also found for mushroom ADH, but are readily accessible to mass spectrometric analyses. Similarly, full-length cDNA segments are not always obtained but also not required when information can be obtained by the combinatorial analyses now used. Crystallography for conformational analyses is of course essential but within a class the similarities are so great for ADH (Table 1; cf. Fig. 3) that conclusions from computer modeling may be useful.

Acknowledgements: Carina Palmberg, Irene Byman and Ulrika Waldenström (this department) are gratefully acknowledged for valuable help and Helena Danielsson-Thorell (Karlstad University) for productive discussions. Financial support from the Swedish Research Council (project 03X-3532), Karolinska Institutet, and the Knut and Alice Wallenberg Foundation (through its Consortium North in Sweden) is gratefully acknowledged.

References

[1] Ohlsson, I., Nordström, B. and Brändén, C.-I. Structural and functional similarities within the coenzyme binding domains of dehydrogenases, (1974) J. Mol. Biol. 89, 339–354.
[2] Rossmann, M.G., Moras, D. and Olsen, K.W. Chemical and biological evolution of a nucleotide-binding protein, (1974) Nature 250, 194–199.
[3] Jörnvall, H. Partial similarities between yeast and liver alcohol dehydrogenases, (1973) Proc. Natl. Acad. Sci. USA 70, 2295–2298.
[4] Nordling, E., Jörnvall, H. and Persson, B. Medium-chain dehydrogenases/reductases (MDR): Family characterizations including genome comparisons and active site modelling, (2002) Eur. J. Biochem. 269, 4267–4276.
[5] Nordling, E., Persson, B. and Jörnvall, H. Differential multiplicity of MDR alcohol dehydrogenases: enzyme genes in the human genome versus those in organisms initially studied, (2002) Cell. Mol. Life Sci. 59, 1070–1075.
[6] Danielsson, O. and Jörnvall, H. 'Enzymogenesis': Classical liver alcohol dehydrogenase origin from the glutathione-dependent formaldehyde dehydrogenase line, (1992) Proc. Natl. Acad. Sci. USA 89, 9247–9251.
[7] Koivusalo, M., Baumann, M. and Uotila, L. Evidence for the identity of glutathione-dependent formaldehyde dehydrogenase and class III alcohol dehydrogenase, (1989) FEBS Lett. 257, 105–109.
[8] Cañestro, C., Albalat, R., Hjelmqvist, L., Godoy, L., Jörnvall, H. and Gonzàlez-Duarte, R. Ascidian and amphioxus *Adh* genes correlate functional and molecular features of the ADH family expansion during vertebrate evolution, (2002) J. Mol. Evol. 54, 81–89.
[9] Danielsson, O., Atrian, S., Luque, T., Hjelmqvist, L., Gonzàlez-Duarte, R. and Jörnvall, H. Fundamental molecular differences between alcohol dehydrogenase classes, (1994) Proc. Natl. Acad. Sci. USA 91, 4980–4984.
[10] Norin, A., van Ophem, P.W., Piersma, S.R., Persson, B., Duine, J.A. and Jörnvall, H. Mycothiol-dependent formaldehyde dehydrogenase, a prokaryotic medium-chain dehydrogenase/reductase, phylogenetically links different eukaryotic alcohol dehydrogenases. Primary structure, conformational modelling and functional correlations, (1997) Eur. J. Biochem. 248, 282–289.
[11] Norin, A., Piersma, S.R., Duine, J.A. and Jörnvall, H. Nicotinoprotein (NAD^+-containing) alcohol dehydrogenase: structural

relationships and functional interpretations, (2003) Cell. Mol. Life Sci. 60, 999–1006.
[12] Shafqat, J., El-Ahmad, M., Danielsson, O., Martínez, M.C., Persson, B., Parés, X. and Jörnvall, H. Pea formaldehyde-active class III alcohol dehydrogenase: Common derivation of the plant and animal forms but not of the corresponding ethanol-active forms (classes I and P), (1996) Proc. Natl. Acad. Sci. USA 93, 5595–5599.
[13] Bradford, M.M. A rapid and sensitive method for the quantitation of microgram quantities of protein utilizing the principle of protein-dye binding, (1976) Anal. Biochem. 72, 248–254.
[14] Parés, X., Cederlund, E., Moreno, A., Hjelmqvist, L., Farrés, J. and Jörnvall, H. Mammalian class IV alcohol dehydrogenase (stomach ADH): Structure, origin and correlation with enzymology, (1994) Proc. Natl. Acad. Sci. USA, 91, 1893–1897.
[15] Giegerich, R., Meyer, F. and Schleiermacher, C. (1996) *GeneFisher* – Software Support for the Detection of Postulated Genes, in: ISMB-96, Proceedings of the Fourth International Conference on Intelligent Systems for Molecular Biology, AAAI Press, New York (ISSN 57735-002-2) 4, 68–77.
[16] Thompson, J.D., Higgins, D.G. and Gibson, T.J. CLUSTAL W: Improving the sensitivity of progressive multiple sequence alignment through sequence weighting, position-specific gap penalties and weight matrix choice, (1994) Nucleic Acids Res. 22, 4673–4680.
[17] Felsenstein, J. Confidence limits on phylogenies: an approach using the bootstrap, (1985) Evolution 39, 783–791.
[18] Sanghani, P.C., Bosron, W.F. and Hurley, T.D. Human glutathione-dependent formaldehyde dehydrogenase. Structural changes associated with ternary complex formation, (2002) Biochemistry 41, 1589–1594.
[19] Abagyan, R.A. and Totrov, M.M. Biased probability Monte Carlo conformational searches and electrostatic calculations for peptides and proteins, (1994) J. Mol. Biol. 235, 983–1002.
[20] Page, R.D.M. Treeview: An application to display phylogenetic trees on personal computers, (1996) Comp. Appl. Biosci. 12, 357–358.
[21] Eklund, H., Plapp, B.V., Samama, J.-P. and Bränden, C.-I. Binding of substrate in a ternary complex of horse liver alcohol dehydrogenase, (1982) J. Biol. Chem. 257, 14349–14358.
[22] Hurley, T.D., Bosron, W.F., Hamilton, J.A. and Amzel, L.M. Structure of human $\beta_1\beta_1$ alcohol dehydrogenase: catalytic effects of non-active-site substitutions, (1991) Proc. Natl. Acad. Sci. USA 88, 8149–8153.
[23] Pietruszko, R. and Theorell, H. Subunit composition of horse liver alcohol dehydrogenase, (1969) Arch. Biochem. Biophys. 131, 288–298.
[24] Danielsson, O., Shafqat, J., Estonius, M. and Jörnvall, H. Isozyme multiplicity with anomalous dimer patterns in a class III alcohol dehydrogenase. Effects of activity and quaternary structure of residue exchanges at 'nonfunctional' sites in a native protein, (1996) Biochemistry 35, 114561–114568.
[25] Hjelmqvist, L., Hackett, M., Shafqat, J., Danielsson, O., Iida, J., Hendrickson, R.C., Michel, H., Shabanowitz, J., Hunt, D.F. and Jörnvall, H. Multiplicity of N-terminal structures of medium-chain alcohol dehydrogenases. Mass-spectrometric analysis of plant, lower vertebrate and higher vertebrate class I, II, and III forms of the enzyme, (1995) FEBS Lett. 367, 237–240.